Optimal Quantum Phase Estimation

U. Dorner,[1] R. Demkowicz-Dobrzanski,[2] B. J. Smith,[1] J. S. Lundeen,[1] W. Wasilewski,[3] K. Banaszek,[2] and I. A. Walmsley[1]

[1]*Clarendon Laboratory, University of Oxford, Parks Road, Oxford OX1 3PU, United Kingdom*
[2]*Institute of Physics, Nicolaus Copernicus University, Grudziadzka 5, PL-87-100 Toruń, Poland*
[3]*Institute of Experimental Physics, University of Warsaw, Hoża 69, PL-00-681 Warsaw, Poland*

By using a systematic optimization approach, we determine quantum states of light with definite photon number leading to the best possible precision in optical two-mode interferometry. Our treatment takes into account the experimentally relevant situation of photon losses. Our results thus reveal the benchmark for precision in optical interferometry. Although this boundary is generally worse than the Heisenberg limit, we show that the obtained precision beats the standard quantum limit, thus leading to a significant improvement compared to classical interferometers. We furthermore discuss alternative states and strategies to the optimized states which are easier to generate at the cost of only slightly lower precision.

Interferometry is one of the most important measurement techniques in physics. Its numerous variations include Ramsey spectroscopy in atomic physics, optical interferometry in gravitational wave detectors, laser gyroscopes or optical imaging to name but a few. All these applications aim to estimate the quantity of interest, normally a relative phase gathered by one "arm" of the interferometer, with highest possible precision. In this Letter, we present fundamental limits to this precision in optical interferometry for light with definite photon number in the presence of losses. To find these limits, it is necessary to consider the "cost" of the experiment, i.e., the required resources, and determine the precision of the estimated phase as a function of the cost. In optical interferometry, the required resource is typically identified to be the number of photons N necessary to reach a desired precision. Classically, the precision of the estimated phase scales then like $1/\sqrt{N}$, the so called standard quantum limit (SQL). Quantum interferometry, on the other hand, promises to beat this limit by employing highly nonclassical entangled states to drastically improve the precision to a scaling $1/N$ known as the Heisenberg limit [1,2]. The realization of interferometric measurements beyond the SQL is a very active field, and recent years have seen tremendous progress [3–7]. A quantum enhancement in precision would allow for a significant reduction of the energy flux while keeping the same measurement precision. This is important, for example, if the phase is induced by a fragile sample [3]. However, most of the theoretical work done so far ignores the unavoidable presence of noise in the system. Existing treatments come to the conclusion that the benefit from highly entangled states deteriorates quickly even if only a small amount of noise is present in the system [8–12]. This is not really a surprise since states of this type are typically very fragile: In optical interferometry, the well-studied $N00N$ state promises to provide Heisenberg limited sensitivity in phase estimation [13];

however, the loss of merely a single photon renders this state useless since it collapses into a product of two Fock states which cannot acquire any phase information.

The Heisenberg limit is believed to be the ultimate precision in optical phase estimation; however, it is yet an unsolved problem if this limit can be reached in the presence of noise and, if not, then what is the ultimate precision? In this Letter, we answer this question for optical two-mode interferometry in the presence of photon losses, which is the limiting source of noise in such experiments. By using a systematic approach, we determine optimal states with definite photon number leading to the highest possible precision. Although it turns out that the Heisenberg limit is unattainable, we show that one can beat the SQL thus greatly improving precision beyond classical interferometry. Furthermore we introduce alternatives to the optimal states, with simpler structure, at the cost of only slightly less precision.

We consider a general interferometer with two arms as shown in Fig. 1; in particular, we do not put any restrictions on the measurement scheme. Channel a is accumulating a phase φ relative to channel b, and both arms, a and b, are subject to photon loss which can be seen as the effect of fictitious beam splitters inserted at arbitrary locations in
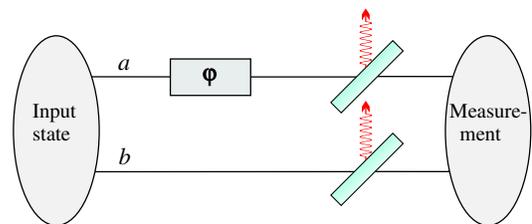

FIG. 1 (color online). General optical interferometric setup with two arms. Channel a acquires a phase φ relative to channel b. The two beam splitters in channel a and b symbolize photon losses.

both channels. We aim to estimate φ with the highest possible precision quantified by using the uncertainty of the estimated phase φ_{est},

$$\delta\varphi = \langle(\varphi_{\text{est}}|\partial\langle\varphi_{\text{est}}\rangle/\partial\varphi|^{-1} - \varphi)^2\rangle^{1/2}, \qquad (1)$$

which, for an unbiased estimator, is simply the standard deviation. According to the general theory of quantum parameter estimation [14–16], $\delta\varphi$ is bounded by the quantum Cramér-Rao bound

$$\delta\varphi \geq \frac{1}{\sqrt{\nu}\sqrt{F_Q}} \equiv \frac{\delta\varphi_{\text{min}}}{\sqrt{\nu}}, \qquad (2)$$

where ν is the number of experimental runs and F_Q is the quantum Fisher information. It was shown that this bound can always be reached asymptotically by maximum likelihood estimation and a projective measurement in the eigenbasis of the "symmetric logarithmic derivative operator" [14]. Hence, inequality (2) defines the *principally smallest possible uncertainty* in phase estimation, the determination of which is the primary scope of this Letter. An explicit construction of the measurement operators will be given elsewhere [17].

Photon losses can be modeled by inserting fictitious beam splitters with transmissivities $\eta_{a,b}$ into both arms of the interferometer which couple the system to (uncorrelated) environments. The noise operation and the phase accumulation commute, i.e., it is irrelevant if photons are lost before, during, or after channel a acquires its relative phase with respect to b. If the noise operation is applied first, the state after tracing out the environmental degrees of freedom can be written as $\rho = \sum_{k,l=0}^{\infty} K_{l,a}K_{k,b}\rho_{in}K_{k,b}^{\dagger}K_{l,a}^{\dagger}$ with Kraus operators $K_{l,a} = (1 - \eta_a)^{l/2}\eta_a^{(1/2)\hat{a}^{\dagger}\hat{a}}\hat{a}^l/\sqrt{l!}$, where $\hat{a}$ is the annihilation operator for mode a, and analogously for mode b. This state acquires a phase through the transformation $\rho(\varphi) = e^{-i\varphi\hat{a}^{\dagger}\hat{a}}\rho e^{i\varphi\hat{a}^{\dagger}\hat{a}}$. This scenario is equivalent to a continuous photon loss model described by a master equation with loss rates $|\ln\eta_{a,b}|$ per unit time.

We consider the most general pure input states with definite photon number N,

$$|\psi\rangle_{\text{in}} = \sum_{k=0}^{N} \alpha_k |k, N - k\rangle, \qquad (3)$$

where $|k, N - k\rangle$ abbreviates the Fock state $|k\rangle_a|N - k\rangle_b$. Special cases of (3) comprise, in particular, the highly entangled N00N state, $(|N, 0\rangle + |0, N\rangle)/\sqrt{2}$, which, in the absence of noise, leads to Heisenberg limited phase estimation but is strongly prone to decoherence otherwise. Equation (3) includes states which are "less" entangled but more robust representing a trade-off between precision and robustness. Also, in the absence of additional reference beams, a superposition of states with different definite photon number would effectively become a mixture [18] of these states. Convexity of F_Q [19] implies then that the

analysis can be restricted to states with definite photon number if we use them successively [17].

In the case of no losses, the state of the system, $|\psi(\varphi)\rangle = e^{-i\varphi\hat{a}^{\dagger}\hat{a}}|\psi\rangle_{\text{in}}$, remains pure, and the quantum Fisher information reads

$$F_Q = 4[\langle\psi'(\varphi)|\psi'(\varphi)\rangle - |\langle\psi'(\varphi)|\psi(\varphi)\rangle|^2]$$
$$= 4[\Delta(\hat{a}^{\dagger}\hat{a})]^2, \qquad (4)$$

where $[\Delta(\hat{a}^{\dagger}\hat{a})]^2$ is the variance of $\hat{a}^{\dagger}\hat{a}$ with respect to the state $|\psi\rangle_{\text{in}}$ and the prime indicates a derivative with respect to φ [14]. In the presence of noise, the pure input state will deteriorate into a mixture $\rho(\varphi)$. If the eigenvalues and eigenstates of $\rho(\varphi)$ are known the quantum Fisher information can be easily calculated [14]. However, very often the analytical diagonalization of $\rho(\varphi)$ turns out not to be feasible. In this case, if the density operator is given in the form $\rho(\varphi) = \sum_j p_j|\psi_j(\varphi)\rangle\langle\psi_j(\varphi)|$, where the $|\psi_j(\varphi)\rangle$ are not necessarily orthogonal, we can use the convexity of F_Q [19] to obtain an upper bound

$$F_Q \leq \tilde{F}_Q = 4\sum_j p_j[\Delta(\hat{a}^{\dagger}\hat{a})_j]^2, \qquad (5)$$

where the variance corresponds to $|\psi_j(\varphi)\rangle$. The bound is reached if the spaces spanned by $\{|\psi_j(\varphi)\rangle, |\psi_j'(\varphi)\rangle\}$ and $\{|\psi_i(\varphi)\rangle, |\psi_i'(\varphi)\rangle\}$ are orthogonal for $j \neq i$. Particularly, we have $F_Q = \tilde{F}_Q$ for the N00N state and, generally, if photon losses are only present in one channel, i.e., $\eta_b = 1$. The latter is relevant if the phase φ is induced by a sample in arm a which also causes the majority of photon losses. Applying Eq. (5) to the state (3), we get

$$\tilde{F}_Q = 4\left(\sum_{k=0}^{N} k^2 x_k - \sum_{l=0}^{N}\sum_{m=0}^{N-l} \frac{(\sum_{k=l}^{N-m} x_k k B_{lm}^k)^2}{\sum_{k=l}^{N-m} x_k B_{lm}^k}\right) \qquad (6)$$

with $x_k = |\alpha_k|^2$ and $B_{lm}^k \equiv \binom{k}{l}\binom{N-k}{m}\eta_a^k(\eta_a^{-1} - 1)^l\eta_b^{N-k}(\eta_b^{-1} - 1)^m$. For $\eta_b = 1$, we have

$$\tilde{F}_Q = F_Q = 4\left(\sum_{k=0}^{N} k^2 x_k - \sum_{l=0}^{N} \frac{(\sum_{k=l}^{N} x_k k B_l^k)^2}{\sum_{k=l}^{N} x_k B_l^k}\right) \qquad (7)$$

with $B_l^k \equiv B_{l0}^k$. Obviously, the phases of the α_k are irrelevant. Furthermore, we proved analytically that $\tilde{F}_Q$ and F_Q are concave functions of the $\{x_k\}$ [17]. This simplifies the numerical maximization of $\tilde{F}_Q$ or F_Q, and, more importantly, it implies that any maximum is global.

Figure 2 shows the results of such an optimization for $\eta_a = \eta_b \equiv \eta = 0.9$ and $\eta_a \equiv \eta = 0.9, \eta_b = 1$, i.e., 10% losses in both arms and one arm, respectively (blue, solid lines). In the following, we concentrate on these two scenarios. The quantity we analyze is $\delta\varphi_{\text{min}} \equiv 1/\sqrt{F_Q}$ (or $1/\sqrt{\tilde{F}_Q}$) corresponding to the best measurement precision for fixed ν [see Eq. (2)]. The lower and upper boundaries of the shaded regions in Fig. 2 are the Heisenberg limit, $1/N$, and a *standard interferometric limit* (SIL) [20] given
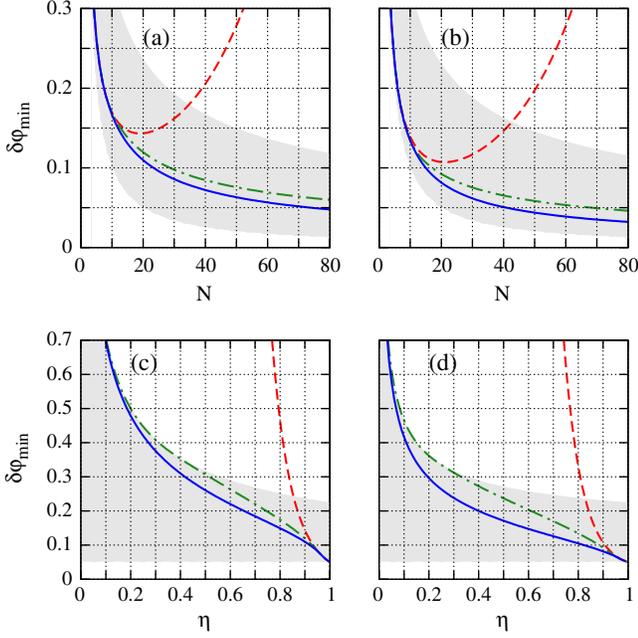
FIG. 2 (color online). Phase estimation precision $\delta\varphi_{\min}$ for losses in both arms of the interferometer (a) versus photon number N ($\eta_a = \eta_b = \eta = 0.9$) and (c) versus transmissivity $\eta_a = \eta_b = \eta$ ($N = 20$). The precision for losses in one arm, i.e., $\eta_b = 1$, is shown in (b) versus N ($\eta_a = \eta = 0.9$) and in (d) versus $\eta_a = \eta$ ($N = 20$). Blue, solid line: Optimal state; Red, dashed line: $N00N$ state; Green, dashed-dotted line: $N00N$ chopping strategy; Shaded area: Region between Heisenberg limit and classical limit (see text).

by $1/\sqrt{N\eta}$ (losses in both arms) and $(1 + \sqrt{\eta})/2\sqrt{N\eta}$ (losses in one arm). Since the SIL is obtained by a classical reference experiment (it scales like the SQL), $\delta\varphi_{\min}$ falling into the shaded region implies an improvement over a classical interferometer. For $\eta_b \neq 1$, we used the state which maximizes $\tilde{F}_Q$ to calculate F_Q which differed by no more than 0.45%. Because of Eq. (5), the "true" maximum has to lie in between these quantities, and its deviation from $\tilde{F}_Q$ can be neglected on the scale given by the difference of the SIL and the Heisenberg limit. As can be seen in Figs. 2(a) and 2(b), it is obviously not possible to reach the Heisenberg limit using input states with definite photon number. However, we gain a significant improvement over the SIL of up to 60% (losses in both arms) and 73% (losses in one arm). The precision for the $N00N$ state in the presence of losses [dashed lines in Figs. 2(a) and 2(b)] is given by $\delta\varphi_{\min} = 1/N\eta^{N/2}$ for losses in both arms and ceases to be optimal for $N > 7$ photons. For losses in one arm, we have $\delta\varphi_{\min} = \sqrt{1 + \eta^{-N}}/\sqrt{2}N$ which is generally worse than the optimal state: Here, it is beneficial to use $N00N$ states with unequal amplitudes of the two components. The best precision of such an "unbalanced" $N00N$ state is given by $(1 + \eta^{-N/2})/2N$ which coincides with the optimal state for $N < 10$. However, for larger

photon numbers, $N00N$ states are not preferable; the precision gets even worse than the SIL.

Figure 3 shows that the optimal state for losses in both arms has generally many nonzero components. Intuitively, this is consistent with the idea that the loss of a photon does not radically change the photon number distribution. The structure of the optimal state is simpler for losses in one arm. We therefore compare it to states with only two nonzero components. The best precision obtained by these states differs by no more than 3% from the optimal case for the example shown in Fig. 2(b). They have the form $\sqrt{p}|m, N - m\rangle + \sqrt{1 - p}|N, 0\rangle$ and are thus similar to the optimal state. This reflects the fact that it is both beneficial to have a large photon number difference between arm a and b and have $m > 0$ so that loss of a photon does not completely destroy the coherence. For equal losses in both arms, the best two-component state has approximately a symmetric form $(|m, N - m\rangle + |N - m, m\rangle)/\sqrt{2}$, but the corresponding precision deviates significantly from the optimal state [up to 13% for the example shown in Fig. 2(a)]. Here, states with more nonzero components are more useful, e.g., a twin Fock state [21] reducing the difference to 9%. Figure 2(c) and 2(d) shows the best possible precision versus η for $N = 20$. For $\eta \gtrsim 0.95 \approx e^{-1/N}$, the optimal state, the optimal two-component state, and the (unbalanced) $N00N$ state are identical.

We can also use different strategies to operate the interferometer: Since our resources are given by the total number of photons, N, we can, instead of employing a single $N00N$ state, use these photons to generate N/n $n00n$ states containing $n \leq N$ photons each, i.e., we split up a "larger" $N00N$ state into a number of "smaller" $n00n$ states which are sent successively through the interferometer. Maximization over n (treated as a continuous parameter) leads to the precision

$$\delta\varphi_{\min} = \begin{cases} \frac{1+\sqrt{\tilde{\eta}}}{2\sqrt{N\eta}}; & \eta \leq \eta_0^{-1} \\ \frac{1+\sqrt{\tilde{\eta}_0}}{2\sqrt{N\tilde{\eta}_0}}\sqrt{\frac{\eta_0|\ln\eta|}{\ln\eta_0}}; & \eta_0^{-1} < \eta \leq \eta_0^{-1/N}, \\ \frac{1+\tilde{\eta}^{N/2}}{2N\eta^{N/2}}; & \eta > \eta_0^{-1/N} \end{cases} \quad (8)$$

where $\tilde{\eta} = \tilde{\eta}_0 = 1$, $\eta_0 = e$ and $\tilde{\eta} = \eta$, $\tilde{\eta}_0 = \eta_0 \approx 4.386$
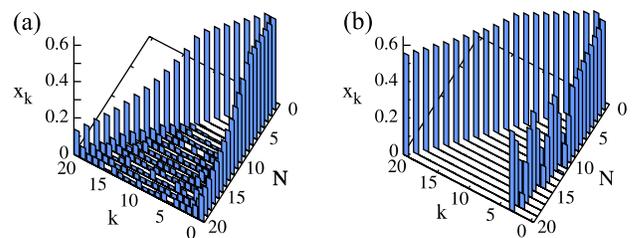

FIG. 3 (color online). Coefficients $x_k = |\alpha_k|^2$ of the optimal state versus photon number N. (a) losses in both arms ($\eta_a = \eta_b = \eta = 0.9$). (b) losses in one arm ($\eta_a = \eta = 0.9$, $\eta_b = 1$).
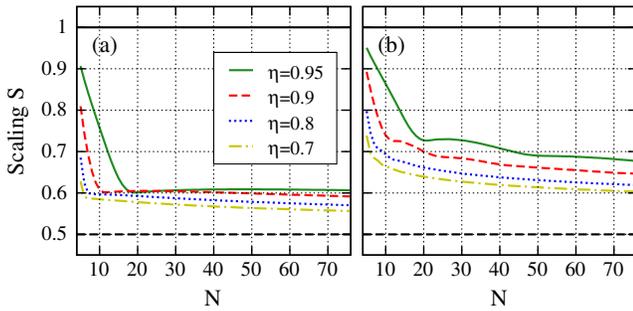
FIG. 4 (color online).   Differential scaling of phase estimation precision $\delta\varphi_{\min}$ with number of photons N for different transmissivities. (a) Optimal state for losses in both arms ($\eta_a = \eta_b \equiv \eta$) and (b) for losses in one arm ($\eta_a \equiv \eta$, $\eta_b = 1$). The color coding is the same in both plots.

for losses in both arms and one arm, respectively. In the latter case, we use unbalanced $n00n$ states. Examples for this "chopping" strategy are given by the green, dashed-dotted lines in Fig. 2. Note that in this case, the total number of experimental runs is $\nu N/n$. The number of photons "per run" is $n = 1$, $n = \ln\eta_0/|\ln\eta|$ and $n = N$ for the three cases in Eq. (8). For sufficiently small total photon numbers [cf. last line in Eq. (8)], it is not an advantage to chop the $N00N$ state. If N is larger, the strategy does not improve the scaling with N compared to the SIL (or SQL). Nonetheless, it is an improvement over the SIL by a constant factor of approximately 2 (losses in both arms) or 2.5 (losses in one arm) in the example shown in Fig. 2, i.e., we need almost four (6.2) times less photons to reach the same measurement precision.

The scaling of the precision of the optimal state with the number of photons turns out not to behave exactly like a power law. Therefore, we define a differential scaling $S(N)$ given by the local slope of $\delta\varphi_{\min}(N)$ on a log-log scale obtained by a linear fit to the points corresponding to $N - 4, \ldots, N + 4$. If $\delta\varphi_{\min}$ scales like a power law S would be the constant power, e.g., $S = 0.5$ for the SQL and $S = 1$ for the Heisenberg limit. Results are shown in Fig. 4. It is clearly visible that the scaling of the optimal state drops quickly, tending away from the Heisenberg limit towards the SQL. Even for rather high transmissivity (green lines correspond to 95%), a scaling of ~0.61 (losses in both arms) or ~0.68 (losses in one arm) for $N = 70$ is not exceeded. Moreover, the scaling gets worse for higher photon numbers. As yet, it remains an unresolved but fascinating question if the scaling of the optimal states eventually tend to the SQL for all $\eta < 1$ or asymptotically reaches a value which beats the SQL proving a true quantum scaling advantage in the presence of losses. Of course these are rather theoretical considerations: In practice there are restrictions to the size of the state (in terms of photon number) which can be experimentally generated. So even if the curves drop to 0.5 for $N \to \infty$, interferometry using "smaller" quantum states has a significant advantage both

in terms of scaling and absolute precision over classical interferometry. Particularly for very small numbers of photons, (unbalanced) $N00N$ states are optimal. Above this threshold, the use of the more complex, optimized states or one of our experimentally more feasible alternatives is favorable.

[1] V. Giovannetti, S. Lloyd, and L. Maccone, Science **306**, 1330 (2004).
[2] V. Giovannetti, S. Lloyd, and L. Maccone, Phys. Rev. Lett. **96**, 010401 (2006).
[3] B. L. Higgins, D. W. Berry, S. D. Bartlett, H. M. Wiseman, and G. J. Pryde, Nature (London) **450**, 393 (2007).
[4] M. W. Mitchell, J. S. Lundeen, and J. S. Steinberg, Nature (London) **429**, 161 (2004).
[5] H. S. Eisenberg, J. F. Hodelin, G. Khoury, and D. Bouwmeester, Phys. Rev. Lett. **94**, 090502 (2005).
[6] T. Nagata, R. Okamoto, J. O'Brien, K. Sasaki, and S. Takeuchi, Science **316**, 726 (2007).
[7] K. J. Resch *et al.*, Phys. Rev. Lett. **98**, 223601 (2007).
[8] S. F. Huelga *et al.*, Phys. Rev. Lett. **79**, 3865 (1997).
[9] A. Shaji and C. M. Caves, Phys. Rev. A **76**, 032111 (2007).
[10] M. Sahovar and G. J. Milburn, J. Phys. A **39**, 8487 (2006).
[11] G. Gilbert, M. Hamrick, and Y. S. Weinstein, arXiv:quant-ph/0612156v1.
[12] S. D. Huver, C. F. Wildfeuer, and J. P. Dowling, arXiv:0805.0296v1.
[13] J. J. Bollinger, W. M. Itano, D. J. Wineland, and D. J. Heinzen, Phys. Rev. A **54**, R4649 (1996).
[14] S. L. Braunstein and C. M. Caves, Phys. Rev. Lett. **72**, 3439 (1994); S. L. Braunstein, C. M. Caves, and G. J. Milburn, Ann. Phys. (N.Y.) **247**, 135 (1996).
[15] C. W. Helstrom, *Quantum Detection and Estimation Theory* (Academic, New York, 1976).
[16] A. S. Holevo, *Probabilistic and Statistical Aspects of Quantum Theory* (North-Holland, Amsterdam, 1982).
[17] R. Demkowicz-Dobrzanski *et al.* (to be published).
[18] K. Mølmer, Phys. Rev. A **55**, 3195 (1997).
[19] A. Fujiwara, Phys. Rev. A **63**, 042304 (2001).
[20] The SIL corresponds to a Mach-Zehnder interferometer with a coherent state of unknown phase and the vacuum at the input ports. This state is equivalent to a statistical mixture of Fock states with Poissonian distribution. For losses in one arm, the beam splitter has to be unbalanced to improve the precision. We note that the SIL is also obtainable by sending successively N single photons through the interferometer.
[21] M. J. Holland and K. Burnett, Phys. Rev. Lett. **71**, 1355 (1993); J. A. Dunningham, K. Burnett, and S. M. Barnett, Phys. Rev. Lett. **89**, 150401 (2002).